Volume 16
Number 8
August 2023
Pages 3169–3624

Energy & Environmental Science

rsc.li/ees

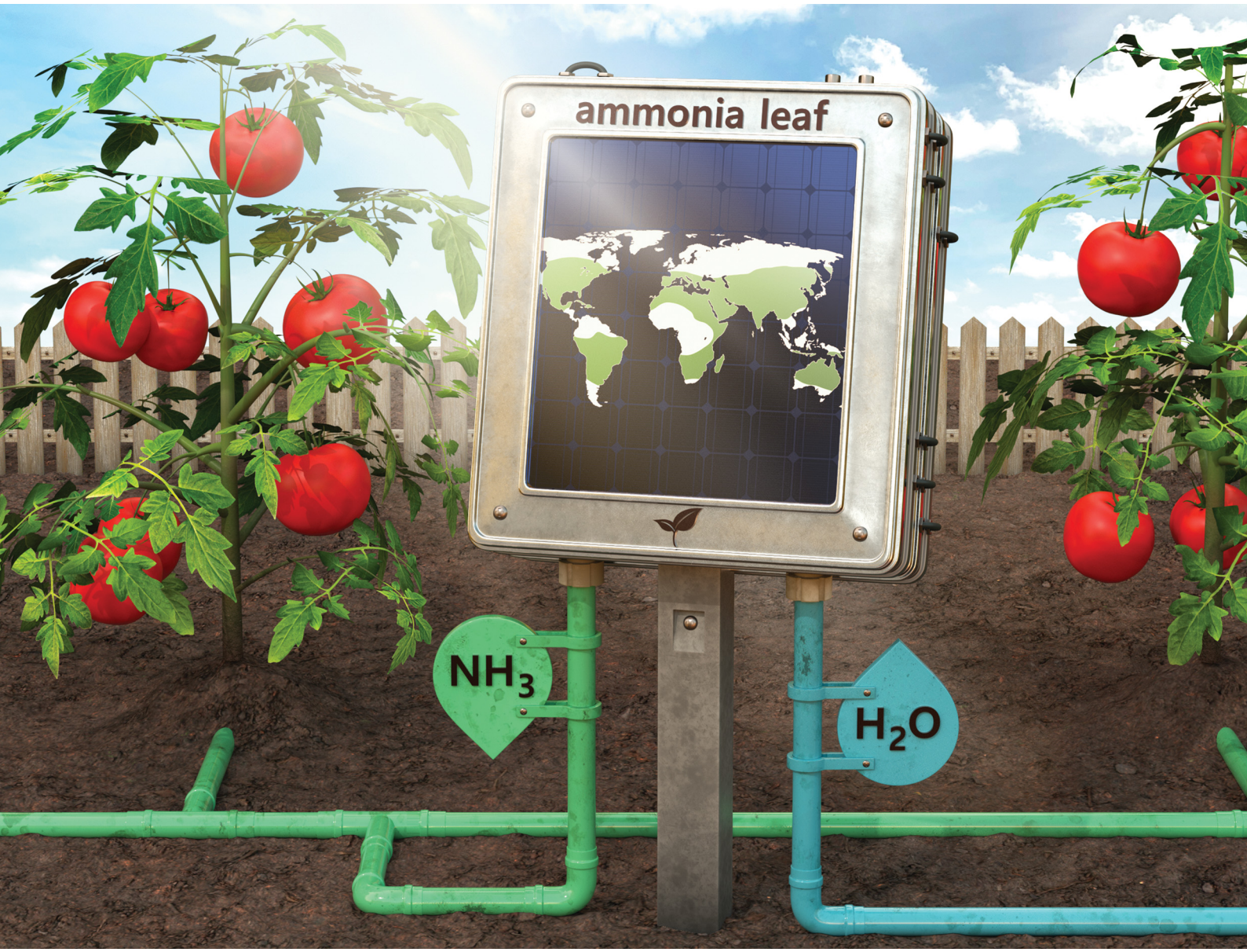

ISSN 1754-5706

ROYAL SOCIETY OF CHEMISTRY

PAPER
Gonzalo Guillén-Gosálbez, Javier Pérez-Ramírez *et al.*
Environmental and economic potential of decentralised electrocatalytic ammonia synthesis powered by solar energy

Energy & Environmental Science

ROYAL SOCIETY OF CHEMISTRY

PAPER

View Article Online
View Journal | View Issue

Cite this: *Energy Environ. Sci.*, 2023, **16**, 3314

Environmental and economic potential of decentralised electrocatalytic ammonia synthesis powered by solar energy†

Sebastiano C. D'Angelo, ‡[a] Antonio J. Martín, ‡[a] Selene Cobo, [a] Diego Freire Ordóñez, [b] Gonzalo Guillén-Gosálbez *[a] and Javier Pérez-Ramírez §*[a]

Received 19th August 2022,
Accepted 20th March 2023

DOI: 10.1039/d2ee02683j

rsc.li/ees

Intense efforts have been devoted to developing green and blue centralised Haber–Bosch processes (gHB and bHB, respectively), but the feasibility of a decentralised and more sustainable scheme has yet to be assessed. Here we reveal the conditions under which small-scale systems (NH_3-leaves) based on the electrocatalytic reduction of nitrogen (eN_2R) powered by photovoltaic energy could realise a decentralised scheme competitive in terms of environmental and economic criteria. For this purpose, we calculated energy efficiency targets worldwide, providing clear values that may guide research in the incipient eN_2R field. Even at this germinal stage, the NH_3-leaf technology would compete favourably in sunny locations for CO_2-related Earth-system processes and human health relative to the business-as-usual production scenario. Moreover, a modest 8% gain in energy efficiency would already make them outperform the gHB in terms of climate change-related impacts in the sunniest locations. If no CO_2 taxation is enforced, the lowest estimated ammonia production cost would be 3 times the industrial standard, with the potential to match it provided a substantial decrease of investment costs and very high selectivity toward ammonia in eN_2R are achieved. The disclosed sustainability potential of NH_3-leaf makes it a strong ally of gHB toward defossilised ammonia production.

Broader context

Ammonia synthesis, typically performed in gigantic Haber–Bosch plants (business as usual, BAU), sustains fertiliser manufacture but is the largest source of CO_2 emissions in the chemical industry. Even though emerging technologies like green hydrogen production and carbon capture and sequestration can alleviate its impact, their environmental benefits are, however, not aligned with economic feasibility to date. A complementary strategy could thus be the creation of a decentralised scheme for on-site ammonia synthesis powered by renewable resources. In this work, we assess its environmental and economic feasibility conceptualising small electrocatalytic reactors for nitrogen reduction in aqueous media coupled to fuel cells and powered by photovoltaic solar energy (coined as ammonia leaf, as it resembles artificial photosynthesis). Geographically-explicit analyses aligned with the planetary boundaries framework revealed regional performance thresholds assuring its environmental competence. We disclose that ammonia leaf could already surpass BAU in most populated regions of the world and parallel other sustainable technologies upon modest technological development. Our analysis also includes conditions under which economic feasibility could be reached. Overall, this study reveals the potential of decentralised solar ammonia synthesis and identifies performance targets for the ammonia leaf technology.

[a] *Institute for Chemical and Bioengineering, Department of Chemistry and Applied Biosciences, ETH Zürich, Vladimir-Prelog-Weg 1, 8093 Zürich, Switzerland. E-mail: gonzalo.guillen.gosalbez@chem.ethz.ch, jpr@chem.ethz.ch*

[b] *Centre for Process Systems Engineering, Imperial College of Science, Technology and Medicine, South Kensington Campus, Roderic Hill Building, London SW7 2BY, UK*

† Electronic supplementary information (ESI) available: Mathematical model, further details on the alternative scenarios compared, further details on the environmental and economic assessment, and further results. See DOI: https://doi.org/10.1039/d2ee02683j

‡ These authors contributed equally.

§ Lead contact.

Introduction

Ammonia is not exclusively seen anymore as the bulk intermediate sustaining the fertiliser industry.[1] Efforts to unlock its potential as an energy carrier are on the rise[2] in electricity generation[3,4] and road[5] and maritime,[6] or even air[7] transportation applications. Realising this future requires, however, an increase in ammonia production by roughly two orders of magnitude to reach volumes comparable to carbon fuel production[8] (current ammonia demand: 182 Mton a^{-1} (~3 EJ a^{-1}), gasoline demand:[9] *ca.* 7000 Mton a^{-1}

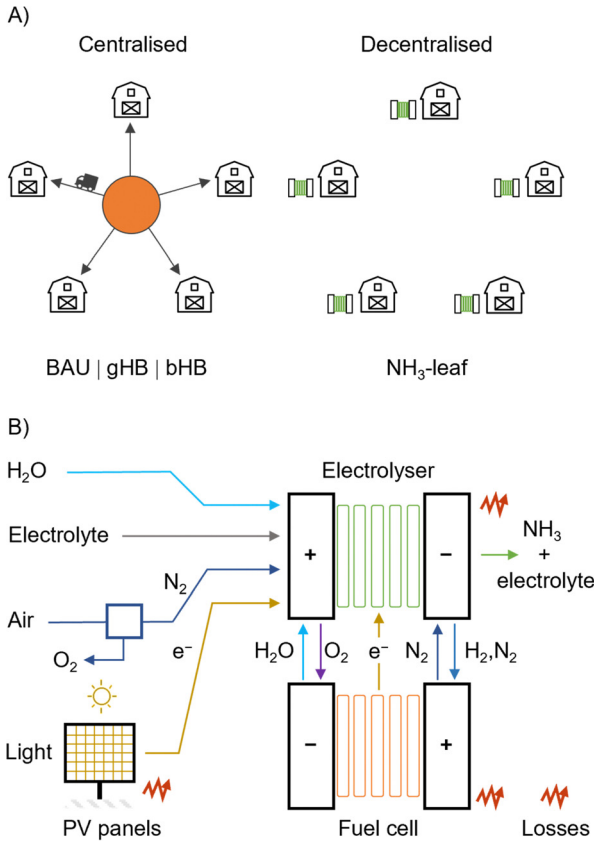

Fig. 1 (A) Simplified representation of a centralised ammonia synthesis scheme, where ammonia would be produced in Haber–Bosch facilities and then distributed to consumers. In contrast, the NH_3-leaf system investigated here would correspond to a decentralised scheme. (B) Schematic representation of the NH_3-leaf considered in this study and auxiliary equipment. Water, electrolyte (0.1 M $KHCO_3$ in this study), air, and light are the required inputs. The electrolyser produces diluted ammonia at the cathodic chamber. A fuel cell fed with the produced hydrogen and oxygen in the electrolyser enables the recycling of electrical energy by valorising these side products to increase the energy efficiency of the overall system. The system is decoupled from the electricity grid.

($\sim$300 EJ a^{-1})). This capacity expansion should follow alternative sustainable pathways to the standard grey ammonia, obtained from the Haber–Bosch (HB) process fed with grey hydrogen from natural gas,[10,11] which shows a large carbon footprint. The more straightforward option is blue ammonia resulting from coupling HB with carbon capture and storage (CCS), known as blue Haber–Bosch (bHB), nonetheless constrained by geological storage limitations.[8,10,12] Among non-fossil alternatives, green Haber–Bosch (gHB) stands out,[2,13,14] based on hydrogen obtained from water electrolysis[10,15–17] (WE) or biomass gasification,[18–20] where the former is gaining momentum due to the incipient commercialisation of water electrolysers.[21,22] These technologies are predicted to sustain the currently deployed centralised scheme of ammonia synthesis based on large-scale plants benefitting from economies of scale (Fig. 1A). The produced ammonia is thus typically transformed into fertilisers, which must later reach end consumers who may be thousands of miles away. Recently, the electrocatalytic reduction of nitrogen[23–25] (eN_2R) emerged as an alternative pathway toward green ammonia, as it could use water as the direct source of protons while operating under mild conditions (*e.g.*, ambient conditions *versus* 100–200 bar and 400–500 °C in the HB reactor). While such a technology, if suitably scaled up, could work in a large centralised setup in connection with the power grid and exploit in particular the low cost of electricity at peak hours, its modularity and special suitability to work directly with renewable energy sources makes it far more appealing on smaller scales, *i.e.*, in a decentralised scheme.[26] Quantifying the currently poorly understood global environmental benefits of these low-carbon ammonia pathways is critical before deploying them at scale.

A number of life cycle assessment (LCA) studies on low-carbon ammonia, covering the shift from grey to centralised blue[16,27–29] and green ammonia,[29–32] highlighted the superior sustainability performance of some low-carbon alternative routes. In particular, a recent LCA study based on the planetary boundary (PB) concept disclosed the potential of green ammonia to substantially reduce the impact on the climate change Earth-system process compared to the fossil HB process. It however revealed the occurrence of burden shifting, *i.e.*, one impact improves at the expense of worsening others in biomass-based routes which could exacerbate the damage to the biosphere integrity.[10] From a technical viewpoint, it was pointed out that producing green ammonia at scale would require large amounts of expensive electrical power in the WE[14–16,33] and in the eN_2R[34–37] routes, making them economically unattractive in the foreseeable future. Specifically, electricity prices as low as 0.025 USD_{2020} kW h^{-1} in a decarbonised grid below 180 g_{CO2} kW h^{-1} (41% lower than the European grid intensity[38]) would be required for centralised green ammonia using WE to become economically and environmentally appealing.[33] Obstacles to centralised green ammonia production *via* eN_2R are even more formidable. Heterogenously catalysed eN_2R in desirable aqueous solvents would need Faradaic efficiencies FE $>$40% at partial current densities for ammonia $>$500 mA cm^{-2} (ref. 33), *i.e.*, a two orders of magnitude increase considering currently attainable performances in state-of-the-art systems like metals and metal oxides, chalcogen- and carbon-based materials or nitrides,[23,39] raising doubts on the practical potential of this route.

Compared to centralised production schemes, decentralised green ammonia could bring additional benefits, particularly in remote locations, taking advantage of regional solar and wind availability, minimising transportation costs and adapting production to specific demands more effectively. In this scheme (Fig. 1A), the sites for production and consumption coincide, targeting small-scale units. Small-scale plants could enable electricity generation when combined with small solid oxide fuel cells,[40] crop fertilisation,[26,41] and automotive fueling. Centralised and decentralised approaches can be understood as complementary strategies with distinctive features, but the potential for the decentralised scheme to contribute to ammonia synthesis remains unknown. Understanding where and to what extent a decentralised scheme should be implemented is thus critical to identifying the best pathways to produce ammonia sustainably.

Here we fill this gap by quantifying the impact of eN_2R coupled with photovoltaics on seven Earth-system processes connected to seven PBs – all of them essential to maintaining the planet's stability defining a safe operating space (SOS) for humanity – alongside the damage to human health, and estimating the production cost. This work explores these production units coined as NH_3-leaves as the first proposition towards the sustainable decentralised synthesis of ammonia. Based on a worldwide solar irradiation atlas, we carry out a spatially explicit sustainability assessment, determining the absolute sustainability performance in each region and providing local breakeven energy efficiencies to compete with centralised alternatives. Our results shed light on the potential role of eN_2R in sustainable development, providing the first figures of merit to guide the development of next-generation electrocatalysts.

Methods

Modelling basis and general assumptions

The ammonia leaf (NH_3-leaf) system implementing the eN_2R technology was assumed to be deployed on a farm able to fertilise one hectare (ha) of wheat, for a total nutrient production target equal to 100 kg N ha^{-1} a^{-1}.[42]

This work expands the original concept of the ammonia leaf system restricted to PV solar panels and an electrolyser.[23,26] The main components of the decentralised NH_3-leaf system, depicted in Fig. 1B, are (i) an electrolyser, which converts water and atmospheric nitrogen into ammonia and hydrogen; (ii) a fuel cell, to reconvert the by-product hydrogen into electrical power and water, thereby reducing the overall electricity and water consumption; and (iii) solar panels supplying the primary electrical power. The modularity of all the system components allows deploying an NH_3-leaf next to the fields fertilised with the produced ammonia. The considered lifespan of the system is 30 years, matching that of solar panels.[43,44] The system instantly attains steady-state conditions when power is available for the electrolyser, *i.e.*, the ramp-up and ramp–down times due to the intermittent energy input are negligible. The NH_3-leaf system is isolated from the electrical grid in this study. Electricity generated by the solar panels is therefore transformed into either chemical energy stored in ammonia, hydrogen or oxygen, or dissipated as losses. In addition to the base scenario described in Fig. 1B, Section S5 in the ESI† also reports two additional scenarios where no fuel cell is considered. In the first of these alternative scenarios, the hydrogen by-product will be vented, and no impact reduction will be attributed to it; the second alternative case considers that the hydrogen would replace the same amount of hydrogen produced *via* proton exchange membrane (PEM) water electrolysis powered by the solar panels assumed for the reference case.

Electrolyser

The electrolyser runs with an aqueous solution and nitrogen entering the cathodic chamber and water at the anodic one. Two reactions occur in parallel, namely, the nitrogen reduction to ammonia (reaction (1)), and the undesired WE (reaction (2)).

$$N_2 + 3H_2O \rightarrow 2NH_3 + \frac{3}{2}O_2 \quad \text{(R1)}$$

$$H_2O \rightarrow H_2 + \frac{1}{2}O_2 \quad \text{(R2)}$$

A polymeric membrane separates anodic and cathodic chambers. A mildly diluted potassium bicarbonate solution (0.1 M $KHCO_3$) was chosen as a representative electrolyte, since it contains elements that can be safely delivered to the crops in such quantity.[45] Related calculations are included in Section S2 of the ESI.† A reverse osmosis pre-treatment unit was included in the system. We considered that 47% of the total water fed to such a pre-treatment unit is converted into high-purity water, which can safely react in the electrolysis cell.[46] Nitrogen is separated from air with a pressure swing adsorption (PSA) unit, which consumes 0.365 kW h kg^{-1} N_2.[47]

The system operates at 25 °C and 1 bar. We consider a theoretical cell voltage U_{th} = 1.17 V to ideally operate nitrogen electroreduction with the oxygen evolution reaction as the anodic half-reaction;[48] moreover, an overpotential of 0.3 V at each electrode[33,49] and an additional ohmic drop of 0.1 V[50] were assumed to calculate the cell voltage. Accordingly, the total voltage efficiency was determined with eqn (1):

$$\eta_V = \frac{U_{th}}{U_{th} + U_{op}} = \frac{U_{th}}{U_{applied}} \quad (1)$$

where η_V is the overall voltage efficiency, defined as the share of the applied energy that is effectively used to produce ammonia and hydrogen, and U_{op} is the total overpotential, calculated as the sum of the overpotentials at the electrodes and the ohmic drop, and $U_{applied}$ is the effectively applied voltage, *i.e.*, the sum of the theoretical voltage and the overpotential. We estimated a voltage efficiency of 63% under these conditions.

We considered different Faradaic efficiencies to ammonia. We accounted for this by computing the ratio of electrical power in reaction (1) to the useful electrical power (η_F). The range of Faradaic efficiencies spanned from a representative figure of the state-of-the art, obtained with a nitrogen-defective carbon nitride-based catalyst (34%),[49] up to 100%. The only considered by-product was hydrogen. The energy conversion efficiency (ECE or η_{ECE}) of the electrolyser can be calculated as follows:

$$\eta_{ECE} = \eta_V \cdot \eta_F \quad (2)$$

This procedure for the calculation of the energy efficiency is equivalent to that for the alternative expression given by the ratio between the reaction enthalpy and electrical energy consumption per mol of product.[51] The lifespan of the unit's active components (electrodes in the case of the electrolyser, and the stack in the case of the fuel cell, including the whole membrane electrode assembly)[52–54] was assumed to be 7 years, after which these components must be substituted and the unit should be subjected to maintenance operations.[52] The total current

density considered in this study was 1.5 A cm^{-2}. It was assumed that the application of gas diffusion electrodes and electrode engineering to eN_2R will substantially increase the currently available current densities (1–10 mA cm^{-2}), reflecting developments in other electrocatalytic technologies such as electrocatalytic CO_2 reduction[55] or polymeric membrane fuel cells.[56]

The product stream contains the electrolyte with dissolved ammonia. To minimise the electrolyte consumption,[57] part of the aqueous ammonia solution is recirculated into the unit. Ammonia was assumed to leave the system at the theoretical limit of 30% w/w.[58] Since the solubility of hydrogen in water is very low, it was separated from the product stream with a flash unit, with a negligible impact on the overall cost.[59] The NH_3-leaf system is deployed at a fully distributed scale for small farms using the ammonia product for fertigation. We assumed that the produced ammonia is deployed as a fertiliser in a 100 ppm solution.[41] Hence, a total of 45.33 L of water are needed to dissolve one kg of ammonia. For example, considering that the diluted ammonia is used to meet the nitrogen demand of wheat –100 kg N ha^{-1} a^{-1} –,[42] the water in the liquid fertiliser would amount to 0.100% of the average irrigation water required by wheat.[60] This fact and the need of diluting the product stream with additional water minimise the risk of soil salinisation due to the use of bicarbonate.[61]

The high-purity oxygen produced at the anode is partially recombined with hydrogen in a fuel cell to reduce the overall system's power consumption. The remaining oxygen was assumed to be vented, avoiding the additional compression costs, as it is unlikely that the global market will be able to absorb it.[59]

Fuel cells

For Faradaic efficiencies below 100%, the produced hydrogen was sent to a fuel cell to generate electrical energy and water. In contrast to the direct injection of hydrogen in the anodic compartment of the electrolyser, the use of a fuel cell enables separate recycling of the hydrogen by-product and thus a stable operation. Hydrogen storage was omitted, under the assumption that the electrolyser and the fuel cell can work under steady-state conditions when the electrolyser is active. We further assumed that the output water from the fuel cell was used in the electrolyser. An average fuel cell efficiency of 60% with respect to the lower heating value of hydrogen was considered.[62] Since this technology has reached an incipient mature stage, only minor improvements in this parameter are expected.[63] A 5-year lifespan was assumed for the active components, after which they should be replaced.[53]

Solar photovoltaic panels

The power provided to the electrolyser was generated with photovoltaic (PV) panels deployed on open ground, with a lifetime of 30 years[43] and a solar-to-power efficiency of 20%.[41] Depending on the location, a solar radiation of 94–281 W m^{-2}, corresponding to an annually averaged incident solar radiation of 2.25–6.75 kW h m^{-2} d^{-1} was considered.[64] At the same time, the PV capacity factors vary from 5.6% to 26.3%,[65,66] based on a global grid of 1140 points, spacing each point by 6° in longitude and 8° in latitude as further described in Section S2 of the ESI.† An average value of 167 W m^{-2} for the incident solar radiation and 11% for the PV capacity factor was selected based on the average PV plant in the ecoinvent database, used in the LCA calculations.[67]

Life cycle assessment

The environmental assessment follows the LCA methodology described in the ISO 14040 and ISO 14044 standards.[68,69]

Phase 1: goal and scope

The first LCA phase is the definition of the goal and scope of the study. Four scenarios were compared: (i) ammonia production *via* the HB process, based on hydrogen derived from natural gas, according to the industrial standard (BAU or grey HB); (ii) the BAU coupled with CCS (blue HB, bHB); (iii) a decarbonised variant of the HB process, where hydrogen is produced through WE powered by PV energy, and nitrogen is obtained from a cryogenic air separation unit (green HB, gHB),[10] and (iv) the NH_3-leaf system described previously. The electricity required in the BAU, bHB and the HB section of the gHB scenario is supplied by the 2019 global average power mix[70] (Table S2, ESI†). To ensure a fair comparison, the gHB scenario implements a water electrolyser powered by PV electricity, with the same PV capacity factors as considered for the NH_3-leaf (see section 'Solar photovoltaic panels'). Furthermore, the system boundaries of all the scenarios include the dilution of ammonia to 100 ppm in an electrolyte solution. The selected functional unit avoids the potential issues that could emerge when comparing the standard fertilization-based approach of the HB-based scenarios with the fertigation-based approach of the NH_3-leaf system. In fact, fertilization-based approaches have been proven to be linked with phenomena of soil and water pollution, which would negatively affect regional nitrogen flows, thus leading to an inaccurate comparison of effects on crops.[71]

The goal of the environmental assessment is to compare the absolute environmental sustainability levels and human health impacts of the assessed technologies. We defined the functional unit as the amount of ammonia that is used to produce fertilisers worldwide (70% of global ammonia production, *i.e.*, 128 Mt in 2019).[72,73] A cradle-to-gate scope based on an attributional approach was adopted, including all the upstream activities and omitting the end-use phase of the final product.

Phase 2: life cycle inventories

We implemented the life cycle inventories (LCIs) of the evaluated ammonia production routes in SimaPro v9.2.[74] Our NH_3-leaf model quantifies the mass and energy flows of the system based on defined efficiencies. The data used to characterise the ammonia electrolyser and the fuel cell are based on previous studies.[75,76] We assumed that the infrastructure requirements and the materials of construction for the ammonia electrolyser, catalyst included, are the same as those of a PEM water electrolyser. The assumption of technological resemblance between nitrogen and water electrolysers has already been

adopted in the analyses of centralised schemes,[34] and is sustained by the similar configuration of most low-temperature electrocatalytic conversion devices, including fuel cells,[77] water,[78] and carbon dioxide electrolysers.[79,80] Previous reports conclude the negligible ecological impact of electrolyser manufacturing.[57,75,81]

The background activities of our model were compiled from ecoinvent v3.5.[67] The LCIs of the grey, blue, and green ammonia processes were sourced from the literature.[10] Additional details about the LCIs, including the energy and water requirements, are provided in Sections S1 and S3 of the ESI.†

Phase 3: life cycle impact assessment

We quantified the impacts of our scenarios on seven Earth-system processes critical to maintaining the planet's stability, namely, climate change, stratospheric ozone depletion, ocean acidification, biogeochemical flows, land-system-change, freshwater use and biosphere integrity. The life cycle impact assessment method we apply allows expressing the environmental impacts in terms of the control variables of the PBs proposed by Steffen *et al.*[82] Our analysis omitted the atmospheric aerosol loading and introduction of novel entities PBs because of methodological gaps. Climate change and biosphere integrity are considered core PBs, *i.e.*, transgressing any of them could drive the Earth into a new state.[82] However, the long-lasting crossing of any PB could trigger the transgression of the core PBs. Thus, the whole set of PBs jointly defines the SOS for humanity.

To quantify the absolute sustainability performance of each route, we proceeded as follows. We first determined the impact of each scenario on the Earth system. Considering the set B of Earth-system processes and the set S of scenarios, the environmental impact of each scenario s in each Earth-system b $\left(\mathrm{EI}_{b,s}^{\mathrm{NH_3}}\right)$ was calculated according to eqn (3):

$$\mathrm{EI}_{b,s}^{\mathrm{NH_3}} = \sum_{e \in E} \mathrm{LCI}_{e,s} \cdot \mathrm{CF}_{b,e} \cdot \mathrm{PV}_{\mathrm{NH_3}} \quad \forall b \in B, \quad s \in S \qquad (3)$$

where $\mathrm{LCI}_{e,s}$ represents the elementary flow e linked to the production of 1 kg of diluted ammonia in scenario s. Note that the values of $\mathrm{LCI}_{e,s}$ are obtained in the second LCA phase (inventory analysis). The parameter $\mathrm{CF}_{b,e}$ denotes the characterisation factor quantifying the impact of elementary flow e on Earth-system process b. These characterisation factors were taken from Ryberg *et al.*[83] for all the Earth-system processes except for the change in the biosphere integrity, for which we used the characterisation factors proposed by Galán-Martín *et al.*[84] derived from ref. 85. Finally, $\mathrm{PV}_{\mathrm{NH_3}}$ denotes the global production volume of ammonia for fertilisers in 2019. We next computed the level of transgression (LT) of each scenario with respect to the SOS. The SOS, which delimits the maximum perturbation that the Earth-system processes can sustain without compromising their long-term stability, is calculated as the difference between the value of the PBs and the natural background levels. Various sharing principles have been proposed to allocate the full SOS among anthropogenic activities,[86] but there is no consensus on which one should be universally applied. Consequently, in this work we did not downscale the global SOS to the production of ammonia, but rather referred the impacts to the full SOS. Hence, we estimated the LT of each scenario $\left(\mathrm{LT}_{b,s}^{\mathrm{NH_3}}\right)$ using eqn (4):

$$\mathrm{LT}_{b,s}^{\mathrm{NH_3}} = \frac{\mathrm{EI}_{b,s}^{\mathrm{NH_3}}}{\mathrm{SOS}_b} \quad \forall b \in B, \quad s \in S \qquad (4)$$

where the environmental impact associated with ammonia production $\left(\mathrm{EI}_{b,s}^{\mathrm{NH_3}}\right)$ is divided by the SOS of each Earth-system process b (SOS_b). When downscaling, a value of $\mathrm{LT}_{b,s}^{\mathrm{NH_3}}$ below 100% implies that the scenario does not exceed the global ecological budget. Conversely, if $\mathrm{LT}_{b,s}^{\mathrm{NH_3}}$ is greater than 100%, then the scenario is unsustainable. Exceeding the ecological budget for at least one of the Earth-system processes implies that the scenario is unsustainable in absolute terms, since the transgression of one single environmental limit can challenge the resilience of the Earth system. However, since here we are considering the full SOS, high values of the LT below 100% do not imply that the technology is sustainable, as it would leave little room for the others to operate within the SOS too. Moreover, we quantified the global warming impacts (or the carbon footprint) of our scenarios expressed in kg CO_2-eq using the ReCiPe 2016[87] method (Hierarchist perspective). We also applied the ReCiPe method (endpoint level) to estimate the human health impacts, measured in disability-adjusted life years (DALYs), which represent the years of healthy life lost. Notably, the resources consumed and the pollutants emitted in our scenarios lead to water use, global warming, fine particulate matter formation, tropospheric ozone formation, stratospheric ozone depletion, ionising radiation, and carcinogenic and non-carcinogenic toxicity, which increase the incidence of certain health risks (*e.g.*, undernutrition, respiratory disease, cancer, *etc.*), damaging human health.

Phase 4: interpretation

Finally, in phase 4, we interpreted the results and made recommendations based on the PBs and human health impacts.

Economic assessment

We compared the total production cost of the studied routes, estimated as the sum of the operational and capital expenditures (OPEX and CAPEX, respectively). The OPEX of the NH_3-leaf system accounts for raw materials, operation of the pressure swing absorption (PSA) unit, end-of-life decommissioning, and operation and maintenance of the solar panels, electrolyser, and fuel cell. The CAPEX was estimated with standard correlations.[43,52,53] In particular, the costs for the electrolyser system were taken from the ones of water electrolysers using a similar PEM technology, under the assumption of a comparable aspirational current density.[88] Such assumption is consistent with the limited influence of current density[33] and electrode material[78] on the CAPEX term. We considered the replacement of active materials for the electrolyser and the fuel cell in the cost calculations. The operating cost of the reverse osmosis pre-treatment unit was considered negligible, since it refers to the energy consumption of a water pump, while the capital expenditure for the unit was included in

the correlation used for the electrolyser cost.[52] Finally, the levelised cost of ammonia (LCOA) was estimated with the methodology and the factors provided in Sections S1 and S4 of the ESI.† The LCOA of the other scenarios was taken from ref. 10 and adjusted by including the product dilution, and the PV capacity factors in the case of gHB.

Results and discussion

Ammonia leaf concept

Our reaction system produces diluted ammonia from water, air, and sunlight under ambient conditions (solar energy was selected over wind power due to its larger potential and milder geographical variability).[89] The system includes a modular eN_2R reactor coupled with photovoltaics based on state-of-the-art components, where the hydrogen by-product is recycled in the form of electrical energy in a fuel cell, expanding the recently coined concept of the ammonia leaf system (NH_3-leaf)[23,26] (Fig. 1 and detailed description in Methods). This system does not require intermediate hydrogen storage, as the input energy from the solar panels is stored as an ammonia solution.

The electroreduction of molecular nitrogen into ammonia with high efficiency in aqueous media is particularly challenging due to the stability of the triple bond and the competing and kinetically facile hydrogen evolution reaction.[90] Overcoming low activity and selectivity to enable eN_2R implementation is the centre of a vibrant research effort spanning the development of accurate testing protocols,[24,50,91] catalyst and reactor design, theoretical efforts[92,93] and process design.[94] These challenges may be, nevertheless, less acute in an NH_3-leaf system. For example, the advantageous use of a diluted stream of ammonia as fertiliser may alleviate the need for high activity[26,41] (and expensive feed purification and product separation steps[95]). In parallel, the conversion of hydrogen into electrical energy may decrease the energy efficiency penalty of low selectivity. The hydrogen by-product could also be used as an energy carrier directly instead of being recycled back as power into the system.

An excellent compromise between sustainability and performance for the envisaged system is found in a defective carbon nitride catalyst, a metal-free material with a high concentration of nitrogen vacancies able to deliver a Faradaic efficiency FE $>30\%$ under *ca.* 300 mV overpotential in aqueous environments.[49] This system was considered as representative of the state-of-the-art for our analysis.

Environmental performance of ammonia synthesis routes

We first study the cradle-to-gate impact of producing the ammonia used for fertilisers worldwide.[72,73] To this end, we compute its greenhouse gas (GHG) emissions (Fig. 2A), impact on seven Earth-system processes (Fig. 2B), and human health damage (Fig. 2C), comparing the NH_3-leaf against the HB process fed with grey hydrogen, blue hydrogen (bHB, based on hydrogen from steam methane reforming with CCS), and green hydrogen (gHB, based on electrolytic hydrogen powered by solar energy). The performance of the solar-dependent technologies (*i.e.*, gHB and NH_3-leaf) varies across locations; therefore, a range of performance levels is provided considering the lowest and highest capacity factors (*i.e.*, ratios of actual yearly power output to ideal annual power output at full capacity) attained by solar photovoltaic (PV) panels,[65,66] as well as current and maximum Faradaic efficiencies.

As expected, the business-as-usual (BAU) scenario deploying grey hydrogen displays a very large carbon footprint, *i.e.*, 290 Mt CO_2 a^{-1}, slightly below the annual GHG emissions of France (Fig. 2A) to put it in context. Consequently, the BAU scenario performs very poorly in the Earth-system processes more closely connected to GHG emissions, *i.e.*, 9.3–9.8% of the SOS in climate change (in the energy imbalance and atmospheric CO_2 concentration control variables, respectively), 3.1% in ocean acidification, and 0.6% in the biosphere integrity (Fig. 2B). In contrast, the impact on the other studied Earth-system processes is negligible ($<0.2\%$); this was in line with our expectations, since all of them, excluding ozone depletion, are mostly connected to agriculture.[96] A prominent feature of this analysis thus emerged: the largest potential benefits of alternative routes *versus* the BAU system will thus emanate from their ability to curb CO_2 emissions. Concerning human health, we found that the BAU's impact amounts to 63 disability-adjusted life years (DALYs) per million people per year, which is, for example, 25% lower than that of acute hepatitis C, ranked as the 127th cause of disease in 2019 by the World Health Organization[97] (Fig. 2C).

Blue ammonia, which still relies on fossil resources, decreases the carbon footprint of the BAU by 72% (Fig. 2A), reducing the climate change and ocean acidification impacts drastically and, to a lesser extent, the damage to terrestrial biosphere integrity (Fig. 2B) and human health (Fig. 2C). However, this route faces issues related to the need for geological storage and the impact of methane leaks.[98,99]

Moving to the gHB, we find that a state-of-the-art water electrolyser (69% efficiency[75]) at the sunniest locations could perform similarly to the bHB (Fig. 2). The situation largely varies when capacity factors drop in regions with less sun availability. In the latter, the larger infrastructure required would lead to small reductions (11–30%) in climate change, ocean acidification and land-system change impacts relative to the BAU, and larger damage to the other Earth-system processes and human health.

The sustainability potential of the NH_3-leaf system becomes evident in all the impact categories, outperforming all other technologies for the best conditions, despite performing the worst in the scenarios with low efficiencies in poorly irradiated regions (Fig. 2). Specifically, the NH_3-leaf system is extremely appealing for high Faradaic efficiencies and high capacity factors, attaining impact reductions in the climate change and ocean acidification Earth-system processes similar to those of the bHB scenario, while leading to further reductions in global warming and human health impacts. All in all, this analysis consistently shows that an NH_3-leaf system may become competitive in environmental and health terms under

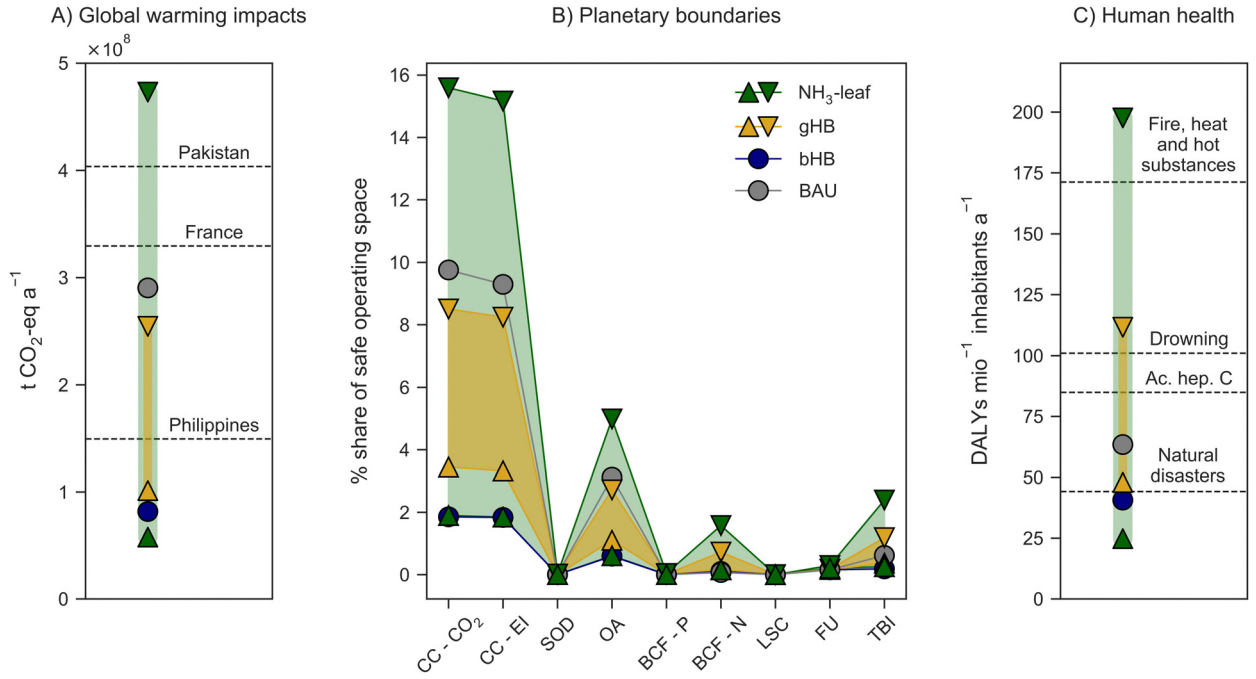

Fig. 2 (A–C) Environmental performance of the four assessed ammonia production technologies, *i.e.*, the ammonia leaf (NH_3-leaf) (green), green Haber–Bosch (gHB) process (yellow), blue Haber Bosch (bHB) process (blue) and business-as-usual (BAU) (grey). In the gHB process, the intervals consider hydrogen produced by solar energy at locations with a capacity factor in the range of 6–26%. Concerning the NH_3-leaf, the values span between a worst-case scenario with 34% Faradaic efficiency and 6% solar capacity factor up to a best case with perfect selectivity and the best (26%) solar capacity factor. Such selection of capacity factors encompasses all the possible terrestrial locations. The voltage efficiency for the NH_3-leaf is fixed at 63%. (A) Global warming impacts, in annual CO_2-eq emissions. The total greenhouse gases annual emissions of selected countries in 2016[101] is reported as dashed horizontal lines. (B) Share of safe operating space for the nine control variables associated with seven analysed Earth-system processes. The naming is as follows: CC–CO_2: climate change – CO_2 concentration; CC-EI: climate change – energy imbalance; SOD: stratospheric ozone depletion; OA: ocean acidification; BCF-N: biogeochemical flows – nitrogen; BCF-P: biogeochemical flows – phosphorus; LSC: land-system change; FU: freshwater use; and TBI: terrestrial biosphere integrity. (C) Human health impacts, in DALYs per million inhabitants per year. The impact associated with the selected health threats is reported as dashed horizontal lines, for the reference year 2019.[97] Acute hepatitis C includes all age groups; fire, heat and hot substances refers to the 15–29 years old age group; drowning is associated with the 50–59 years old age group; and natural disasters includes the 30–49 years old age group.

certain conditions, ultimately enabling a more sustainable ammonia-based economy.

The previous analysis reveals the high sensitivity to the location and Faradaic efficiencies that the sustainability of an NH_3-leaf system exhibits. Hence, we next determined, for the best and worst locations, the minimum energy conversion efficiency (ECE) required for an NH_3-leaf system to outperform other technologies (breakeven efficiency). To this end, considering a

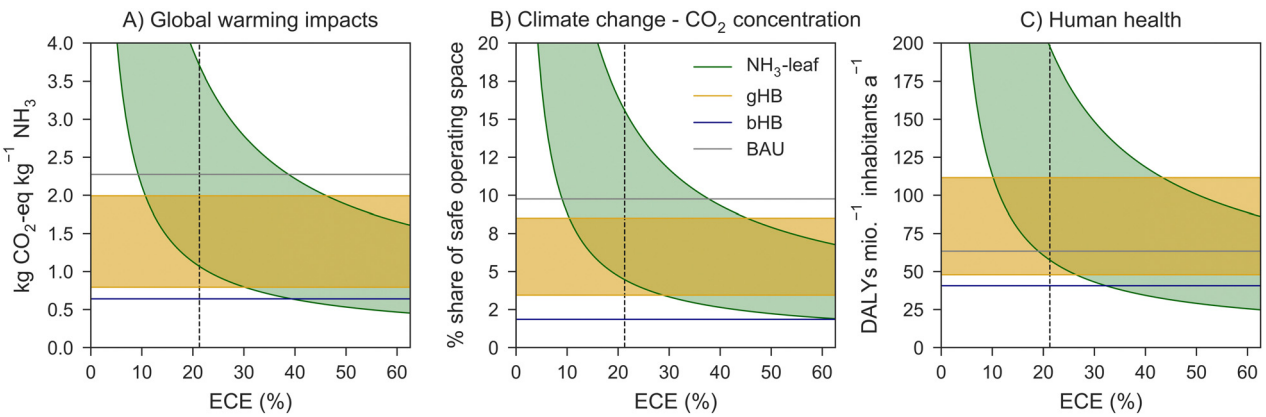

Fig. 3 (A–C) Map showing the environmental impacts of the ammonia leaf system (NH_3-leaf, green) on three selected metrics *versus* the total energy conversion efficiency (ECE), compared with Haber–Bosch processes, namely, green Haber–Bosch (gHB, yellow), blue Haber–Bosch (bHB, blue), and business-as-usual (BAU, grey). The voltage efficiency was kept constant at 63%, while the Faradaic efficiency was varied. The solar capacity factors considered are 6–26%, for both the NH_3-leaf and gHB scenarios. Such selection of capacity factors encompasses all the possible terrestrial locations.

state-of-the-art hydrogen-to-power fuel cell efficiency (60%),[62] we vary the ECE of the NH_3-leaf system for the lowest and highest capacity factors, determining its impact across plausible locations (green area in Fig. 3, where the currently attainable ECE of 21% is indicated with a vertical dashed line). In Fig. 3, the performance of the gHB process is represented by the yellow area delimited by the worst and best locations. The impacts of the BAU and bHB are independent of the region and ECE and are, thus, represented by horizontal lines. The breakeven efficiency of the NH_3-leaf with respect to a given technology at a specific location is given by the intersection between the performance lines of the two technologies. At present, the NH_3-leaf technology would already outperform the BAU in climate change and human health at the best location (9–53% less impact). Remarkably, ECEs of only 29% and 26% would be needed in the sunniest areas to outperform the gHB in climate change and human health, respectively, while much higher efficiencies would be required to surpass the bHB (>65% in climate change and 32% in human health). These performance requirements are predicted to drop as the economy is decarbonised and the carbon footprint of solar energy declines up to 7.5 times with new-generation PV technologies.[100]

The inspection of impact curves in Fig. 3 for the NH_3-leaf system suggests rapid gains in the near term. Specifically, a sharp decrease in impact occurs with increasing efficiencies at low efficiency values, followed by stabilisation at high efficiencies, indicating that efficiency gains become milder as maturity is reached. Rapid gains are thus still achievable, as the current state-of-the-art is located at the transition between the two regimes. This feature is even more strongly highlighted if optimistic future estimates for the system energy losses of the solar-powered alternatives (see Fig. S5 in the ESI†) or even ideal zero losses at a stack level (compare Fig. S3 in the ESI†) are considered. Furthermore, if a configuration without a fuel cell is considered, the impacts increase when hydrogen is vented, because of the higher energy consumption (see Fig. S8, ESI,† *e.g.*, a carbon footprint of 1.07 kg CO_2-eq kg^{-1} NH_3 for an ECE of 21% in the base case with the best capacity factor, and 1.14 kg CO_2-eq kg^{-1} NH_3 in the corresponding case without a fuel cell). Conversely, the attribution of avoided impacts to the hydrogen by-product can lead to a decrease in total impact. We note that such credits are questionable, as they imply that the required infrastructure to store and use the generated hydrogen would be available. Continuing with the analysis of impact curves, we find that they display very similar shapes, suggesting a common driver. The breakdown of impacts in Fig. S7 available in the ESI† discloses the consumption of renewable energy as the predominant source of impact, as solar panels are the main contributors (>67%), followed at a distance by the electrolyser construction (3–8%), excluding the contribution associated with the electrolyte solution that is incorporated into the product stream.

The contribution of the stack construction is thus marginal, and, since a PEM electrolyser was assumed as proxy for the materials with inclusion of platinum- and iridium-based catalysts, this can be considered as a conservative estimate. A sensitivity analysis displayed in Fig. S2, ESI† confirms the limited influence of the electrolyser and fuel cell stack construction on the environmental impacts. Furthermore, the stark predominance of electricity consumption is also highlighted by performing a sensitivity analysis on the voltage efficiency, with carbon-related and human health impacts showing a pronounced variation with respect to this parameter (Fig. S1A in the ESI†). Such a stark dependence on the energy consumption of the system is reflected in the values of overall system efficiencies associated with the different cases, *i.e.*, the efficiencies that account for the ratio of the LHV of ammonia and the total energy consumption of the different systems. For example, the NH_3-leaf system is not environmentally competitive with gHB at the best location if state-of-the-art ECE is considered. Such an observation is mirrored by a higher overall system energy efficiency of the gHB case, with a value of about 50%,[102] against 34% for the total NH_3-leaf system comprising not only an electrolyser but also a fuel cell. If, however, an ECE of 44% is considered, the energy efficiency of the NH_3-leaf system with fuel cell reaches *ca.* 50%, matching the gHB in terms of energy efficiency and outperforming it in environmental impacts at most locations.

Benefits of the ammonia leaf system in populated areas

To gain further insight into the locations where the decentralised NH_3-leaf scheme could become competitive, we next performed a spatially-explicit environmental analysis considering regional sun power availability (Fig. 4). We first built an atlas of PV capacity factors with a 668 × 889 km^2 granularity (at the equator), with values ranging from 5.6% in the Antarctic ocean (65° S, 160° W) to 26.3% in the Atacama desert (24° S, 69° W), and an average value of 11.0% across all locations (Fig. 4A). We then computed the range of impact values that would be attained in climate change (Fig. 4B) and human health impacts (Fig. 4C) at every potential location for a range of energy conversion efficiencies (*i.e.*, from the current one, 21%, to 63%, corresponding to a 100% Faradaic efficiency, see Methods). Local breakeven ECEs relative to the BAU were then calculated for the climate change (Fig. 4D) and human health (Fig. 4E) impacts of the NH_3-leaf system.

Our analysis reveals that many densely inhabited locations show breakeven efficiencies close to the current reference value. For instance, the breakeven efficiencies in Madrid, Sao Paulo, Sidney, Hong Kong, or Chennai and the surrounding areas vary within 10.4–12.1% for climate change, and 22.1–26.1% for human health (relative to the BAU). Moreover, NH_3-leaves with very high Faradaic efficiency could surpass the gHB in climate change and human health, and could outperform the bHB but only in human health (Fig. 4F and G).

An equally important reading is the stark regional variation of breakeven efficiencies between *ca.* 10 and 60% depending on the capacity factors (Fig. 4D and E), enabling the gradual geographical penetration of an NH_3-leaf system as it reaches maturity. Table 1 summarises the figures of merit to guide the development of eN_2R electrocatalysts for the NH_3-leaf system. Given a breakeven ECE, we determine the more easily attainable Faradaic efficiency toward ammonia, leading to target

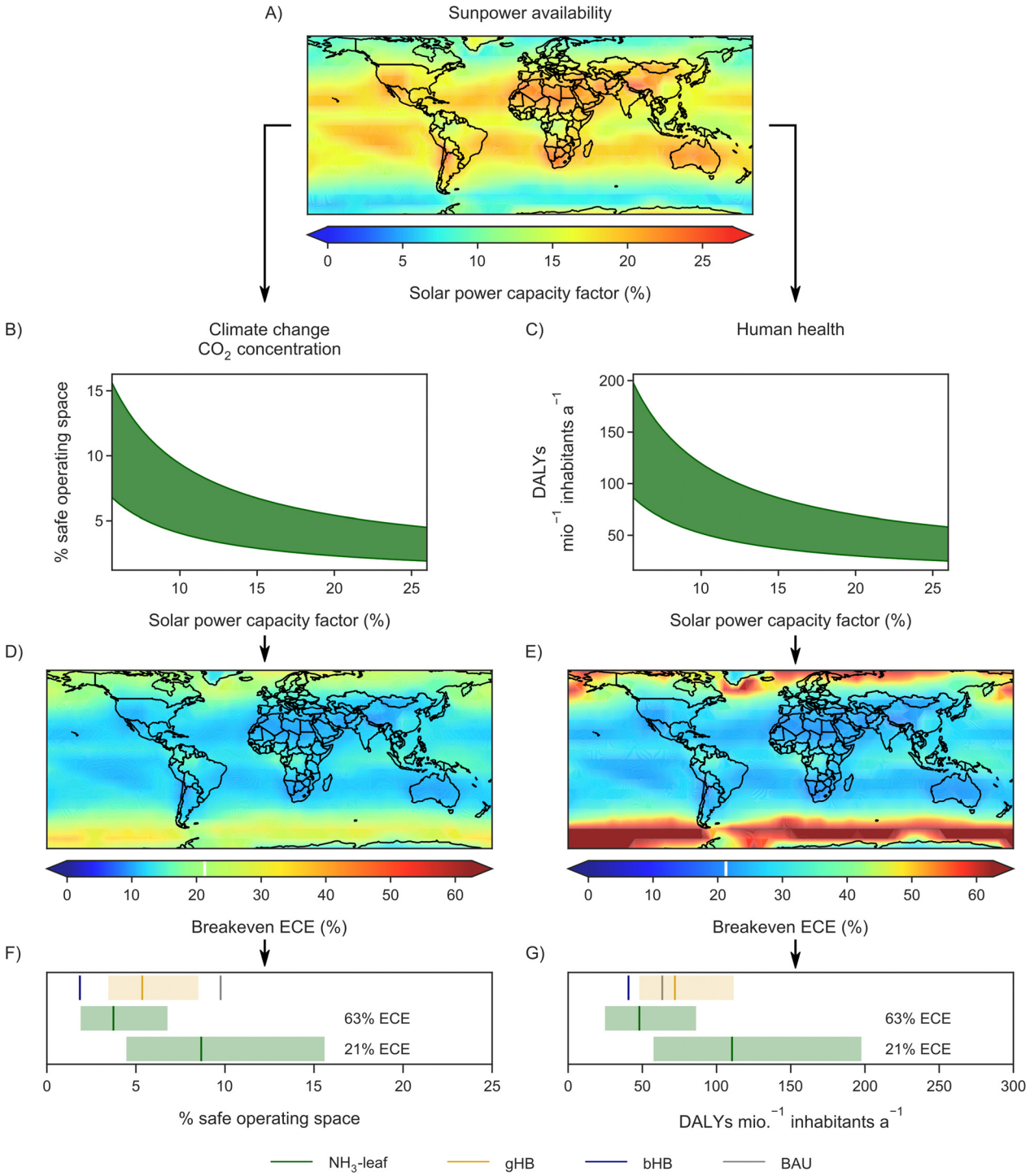

Fig. 4 (A) Global distribution of solar power capacity factors. The capacity factors span the range 6–26% across the possible terrestrial locations. The average global capacity factor (11%) is represented by the green colour. (B and C) (B) Climate change – CO_2 concentration and (C) human health impacts as a function of the solar power capacity factor, assuming energy conversion efficiency (ECE) values in the range of 21–63%. (D and E) Maps showing breakeven ECEs for the ammonia leaf (NH_3 leaf) relative to the current BAU for (D) climate change – CO_2 concentration and (E) human health impacts. The green colour also corresponds to the average global capacity factor and the white lines in the color scales mark the reference value considered in this work (21%). (F and G) Sensitivity ranges comparing the environmental performance in (F) climate change – CO_2 concentration and (G) human health for the NH_3 leaf at the current best Faradaic efficiency (34%, green bottom range), the NH_3-leaf at maximum Faradaic efficiency (100%, green top range), the green Haber–Bosch (gHB, yellow), the blue Haber–Bosch (bHB, blue), and the business-as-usual (BAU, grey). The ranges are given by the lower and upper bounds on solar capacity factors (6–26%), while the lines in the ranges correspond to the average global capacity factor (11%) for the cases based on solar electricity.

Table 1 Range of figures of merit based on environmental assessments for the development of NH_3-leaves

Breakeven energy efficiency (%)	Faradaic efficiency NH_3[a] (%)
10	16
20	32
30	48
40	63
50	79
60	95
63	100

[a] 0.3 V cathodic and anodic overpotentials and 0.1 V ohmic drop.

values between 16 and 100%. In view of the previous analysis, it is possible to claim that an electrolyser operating at 48% Faradaic efficiency with 0.3 V cathodic overpotential (*i.e.*, 30% ECE) would be advantageous across almost all populated areas of the Earth.

Conditions for economic feasibility of ammonia leaf

We finally analyse the levelised cost of ammonia (LCOA) of all the studied technologies (Fig. 5), considering from the worst to the best PV capacity factor, and ECEs up to the maximum of 63% attainable under our assumptions (100% Faradaic efficiency, see Table 1; see also Fig. S4 in the ESI† for the same results considering a voltage efficiency of up to 100%). The first noticeable result is the substantial gap between fossil carbon-based (BAU and bHB) and non-fossil carbon-based (gHB and NH_3-leaf) technologies. The BAU attains the lowest LCOA (0.62 USD_{2020} kg^{-1} NH_3), followed by the bHB (0.66 USD_{2020} kg^{-1} NH_3), while at the best locations the gHB would lead to 1.85 USD_{2020} kg^{-1} NH_3 and state-of-the-art NH_3-leaves, to 5.97 USD_{2020} kg^{-1} NH_3. However, in the best case (100% Faradaic efficiency at the best location), the LCOA of NH_3-leaf would drop to 1.63 USD_{2020} kg^{-1}, outperforming the gHB. Nevertheless, the perspective changes if, instead of considering stable natural gas production prices, we re-calculate the BAU using spikes in spot prices for fossil feedstock, as in Europe in August 2022:[103] by increasing the feedstock cost by 10 times, the corresponding production cost increases by 3.4 times. In this scenario, an ECE of 51% at the best location would be sufficient to make the NH_3-leaf competitive with the BAU. In addition to this, if future reductions of energy losses at a system level could further drive down the energy consumption of both the solar-dependent routes, comparable costs for the two routes would still be obtained in the best cases, but with a less pronounced gap. For example, assuming a 10% improvement in the stack efficiency of PEM electrolysis and about 12% improvement in the voltage efficiency of the NH_3-leaf, gHB could show a LCOA lower than the best case for NH_3-leaf by about 0.09 USD_{2020} kg^{-1} NH_3 (see Fig. S6 in the ESI†). Based on these results, we computed a minimum carbon tax from *ca.* 553 to 5192 USD_{2020} t^{-1} CO_2-eq (*ca.* 7–69 times the CO_2 border tax expected in the European Union in 2026[104]) for the NH_3-leaf to break even economically with the fossil-based routes. Hence, the need for technology development and regulatory intervention is clear to pave the way toward the implementation of the NH_3-leaf system.

The cost breakdown of an NH_3-leaf (Fig. 6A and B) reveals that the capital expenditures (CAPEX) linked to the electrolyser, fuel cell, and PV panels dominate the total cost (~66–77%) in all cases, clearly surpassing the operating expenditures (OPEX) even in the most favourable case of the minimum PV surface and absence of a fuel cell (Fig. 6B). At the same time, the stark dominance of solar PVs over the total cost is confirmed by a sensitivity analysis on the capital costs of the three main components of the NH_3-leaf system, the overall cost of which

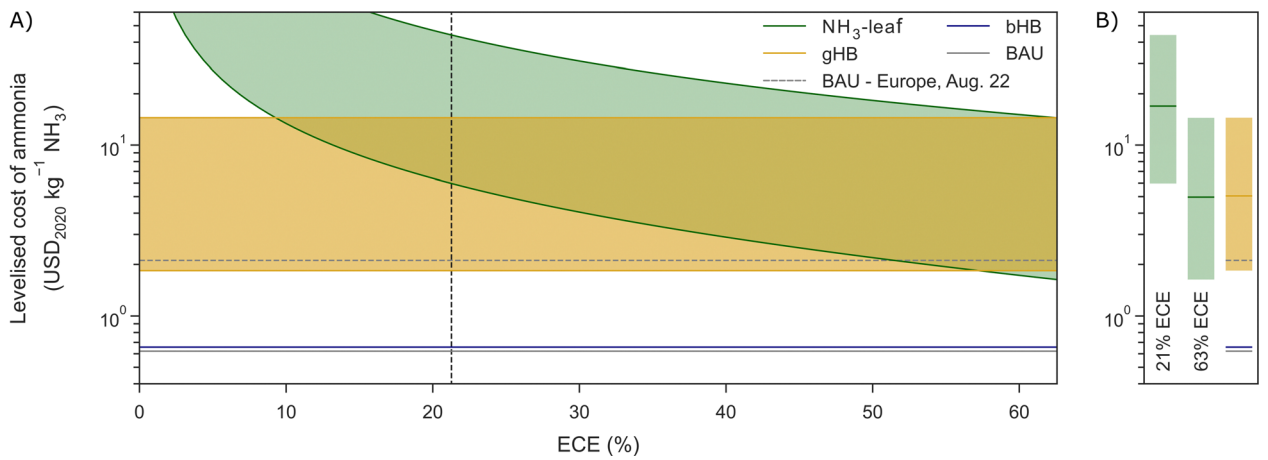

Fig. 5 (A and B) Economic performance of the ammonia leaf (NH_3-leaf) concept. The colour scale is consistent with previous figures, with the NH_3-leaf depicted in green, green Haber–Bosch (gHB) in yellow, blue Haber–Bosch (bHB) in blue, and business-as-usual (BAU) in grey. The grey dashed line represents the BAU re-calculated when assuming a cost of natural gas feedstock equal to the purchase prices in Europe in August 2022, *i.e.*, *ca.* 10 times higher than the cost assumed for the reference case (grey solid line). (A) Sensitivity of levelised cost of ammonia, in USD_{2020} kg^{-1}, with respect to the energy conversion efficiency (ECE). The NH_3-leaf range spans from a worst-case scenario with a 6% solar capacity factor to a best-case scenario with a 26% solar capacity factor. The voltage efficiency was kept constant at a value of 63%, while the Faradaic efficiency was varied. (B) Sensitivity ranges comparing the economic performance of the NH_3-leaf concept with selected technologies. The ranges are given by the lower and upper bounds on solar capacity factors (6–26%), while the lines in the ranges correspond to the average global capacity factor (11%) for the cases requiring solar electricity. Such selection of capacity factors and associated areal energy densities encompasses all the possible terrestrial locations.

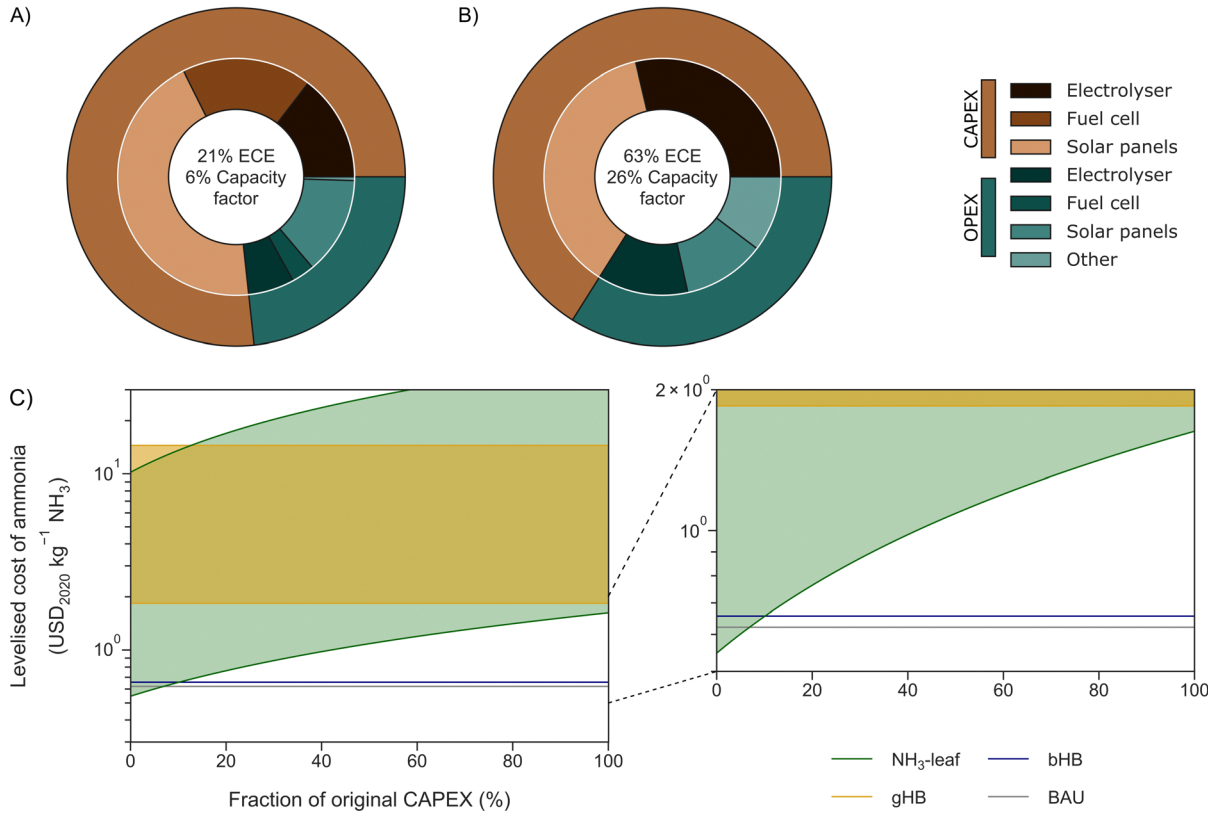

Fig. 6 (A and B) Breakdown of levelised cost of ammonia into its main components: capital expenditures (CAPEX, brown) and operational expenditures (OPEX, blue), divided into electrolyser, fuel cell, solar panels, and other components. The category "Other" includes water and electrolyte requirements to operate the system. The voltage efficiency of the electrolyser was fixed at 63%, while the Faradaic efficiency, and, thus, the energy conversion efficiency (ECE), and the solar capacity factor were varied between the worst (A) and best (B) scenarios. (C) Sensitivity of the levelised cost of ammonia, in USD_{2020} kg^{-1}, with respect to the capital investment (CAPEX). The operating expenditures associated with operation and maintenance were kept constant, while the capital investment, including the replacement costs for the electrolyser and fuel cell, was varied. The colour code is the same as in the previous figure, with the upper green line representing the ammonia leaf (NH_3-leaf) technology with 34% Faradaic efficiency and a 6% capacity factor, and the lower line of the same colour corresponding to the scenario with a 100% Faradaic efficiency and 26% capacity factor. The yellow shaded area represents the deployment of the green Haber–Bosch (gHB) option under the solar capacity factor range of 6–26%. Such selection of capacity factors and associated areal energy densities encompasses all the possible terrestrial locations. Blue and grey lines represent the blue Haber–Bosch (bHB) and the business-as-usual (BAU) strategies, respectively.

is strongly dependent on the electricity generation (Fig. S1B, ESI†). The electrolyser and fuel cell play a more significant role when analysing the overall costs. In the scenario without a fuel cell, the overall cost declines because the avoided purchase of the extra unit overshadows the increased costs associated with the additional energy consumption, as discussed in more detail in the ESI† (see Fig. S9, ESI† and associated discussion). Prospects indicate that the capital cost of hydrogen electrolysers, here taken as the reference value to cost the ammonia one, may drop below 50–82% in the long term,[105] while the CAPEX of fuel cells and solar panels could decrease 35%[106] and 50% within 30 years,[107] respectively. These trends will be accompanied by higher Faradaic efficiencies and current densities in the electrolysers, which, together with the use of less expensive materials, will enable smaller and less costly units.

A sensitivity analysis of the CAPEX cost contributor shows that these improvements could greatly reduce the LCOA of NH_3-leaf, *e.g.*, halving the CAPEX would result in an LCOA of 1.1 USD_{2020} kg^{-1} NH_3 (100% Faradaic efficiency and the highest capacity factor), or 3.74 USD_{2020} kg^{-1} NH_3 (current Faradaic efficiency and the highest capacity factor). Yet, matching the LCOA of the BAU and gHB in the absence of CO_2 taxation would require a very demanding ~90% reduction in capital costs and 100% Faradaic efficiencies concurrently (Fig. 6C), reinforcing the need to define incentives to promote this technology.

Criteria for technology selection and outlook

We finally combine the environmental and economic analyses of all the considered technologies to provide a unified view of the competence of the NH_3-leaf concept.

The radar plot shown in Fig. 7 represents the range of environmental impacts and levelised cost of ammonia across all locations, giving rise to the observed bands for gHB and NH_3-leaf. The ECE of the NH_3-leaf was here fixed to 63% (100% Faradaic efficiency and 63% voltage efficiency) (see Methods). A quick inspection discloses the unbalanced nature of the BAU, overall underperforming all other alternatives in environmental

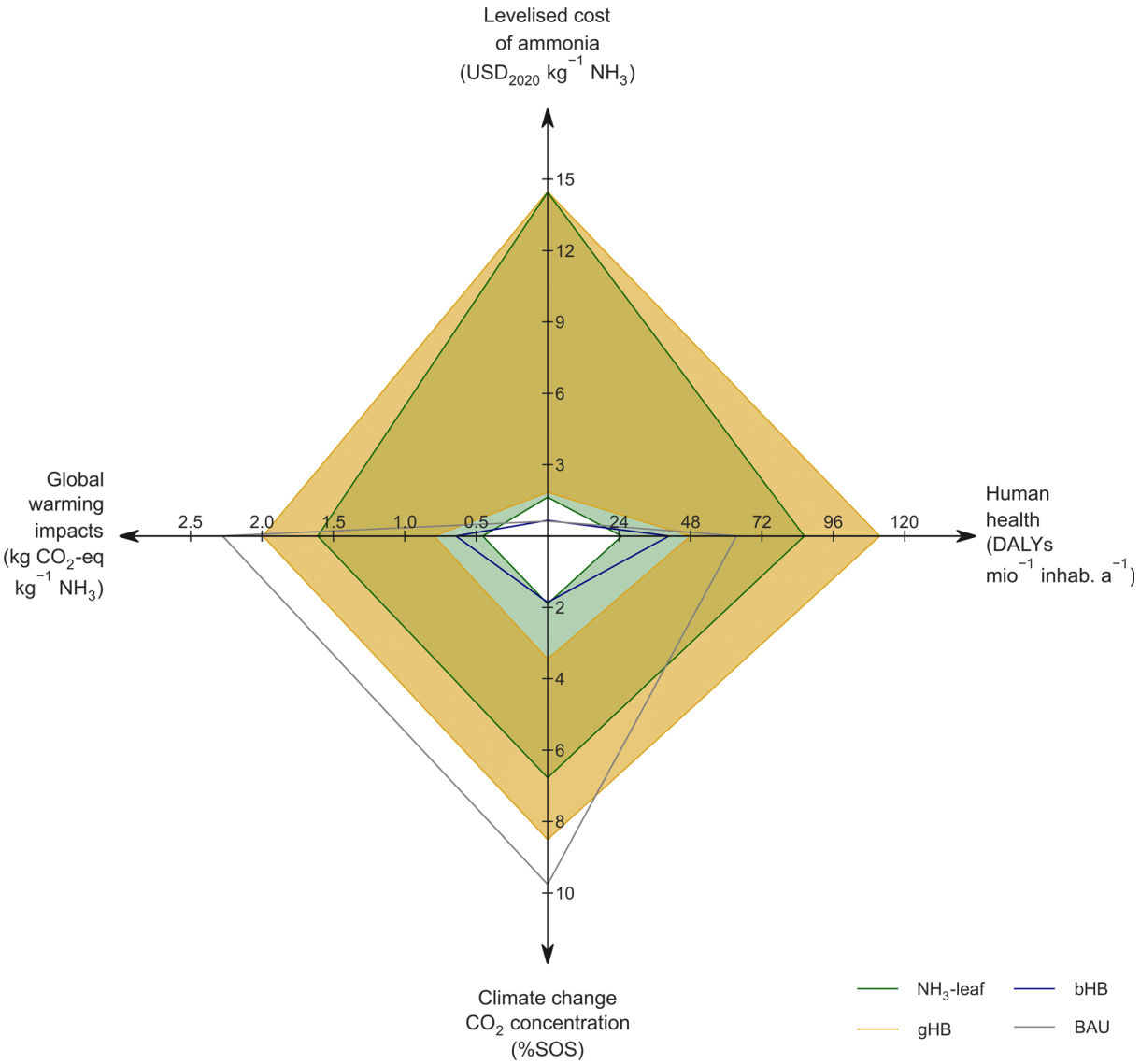

Fig. 7 Summary of figures of merit drawn from the comparison of the ammonia leaf (NH_3-leaf, green area) with the green Haber–Bosch (gHB, yellow area), blue Haber–Bosch (bHB, blue line), and conventional Haber–Bosch (BAU, grey line). The green range represents the performance of the NH_3-leaf at 100% Faradaic efficiency and 63% voltage efficiency, varying only the solar capacity factor in the range 6–26%. Such selection of capacity factors and associated areal energy densities encompasses all the possible terrestrial locations. The yellow area represents the impact of the gHB scenario with a solar capacity factor within the same range as the NH_3-leaf. Small scores represent high performance for all axes.

terms at the best locations but showing the minimum levelised cost.

The inclusion of CCS in the bHB balances both aspects, allowing it to display consistently low values across all considered parameters. bHB could thus be considered as the preferable option as long as CO_2 storage capacity is available. As for the decarbonised alternatives, the large overlap between gHB and NH_3-leaf highlights that both are complementary and that the optimal technology mix will depend on the location and maturity of the NH_3-leaf. Nevertheless, assuming the highest ECEs at the sunniest locations, where impacts and levelised cost are minimum, the figure discloses that highly performing NH_3-leaves would be preferred, as they would exhibit lower impacts at a similar levelised cost.

The procedure developed so far could thus be expanded upon a comprehensive consideration of local features affecting environmental and economic performance to select the most beneficial technology for every location. The first step towards this direction is given in Fig. 8, where the impact on climate change – CO_2 concentration for the case of the NH_3-leaf reaching a realistic target of 55% FE and state-of-the-art gHB is analysed in Fig. 8A. Based on this, either the NH_3-leaf or gHB is selected for every analysed terrestrial location based on which of the two shows the lowest impact in this impact category. This analysis shows how the NH_3-leaf would be the technology of choice for warm and temperate latitudes, whereas gHB would be preferable for cold ones, except in some equatorial regions where the average solar irradiation decreases due to the common presence of clouds (see also Fig. 8B).

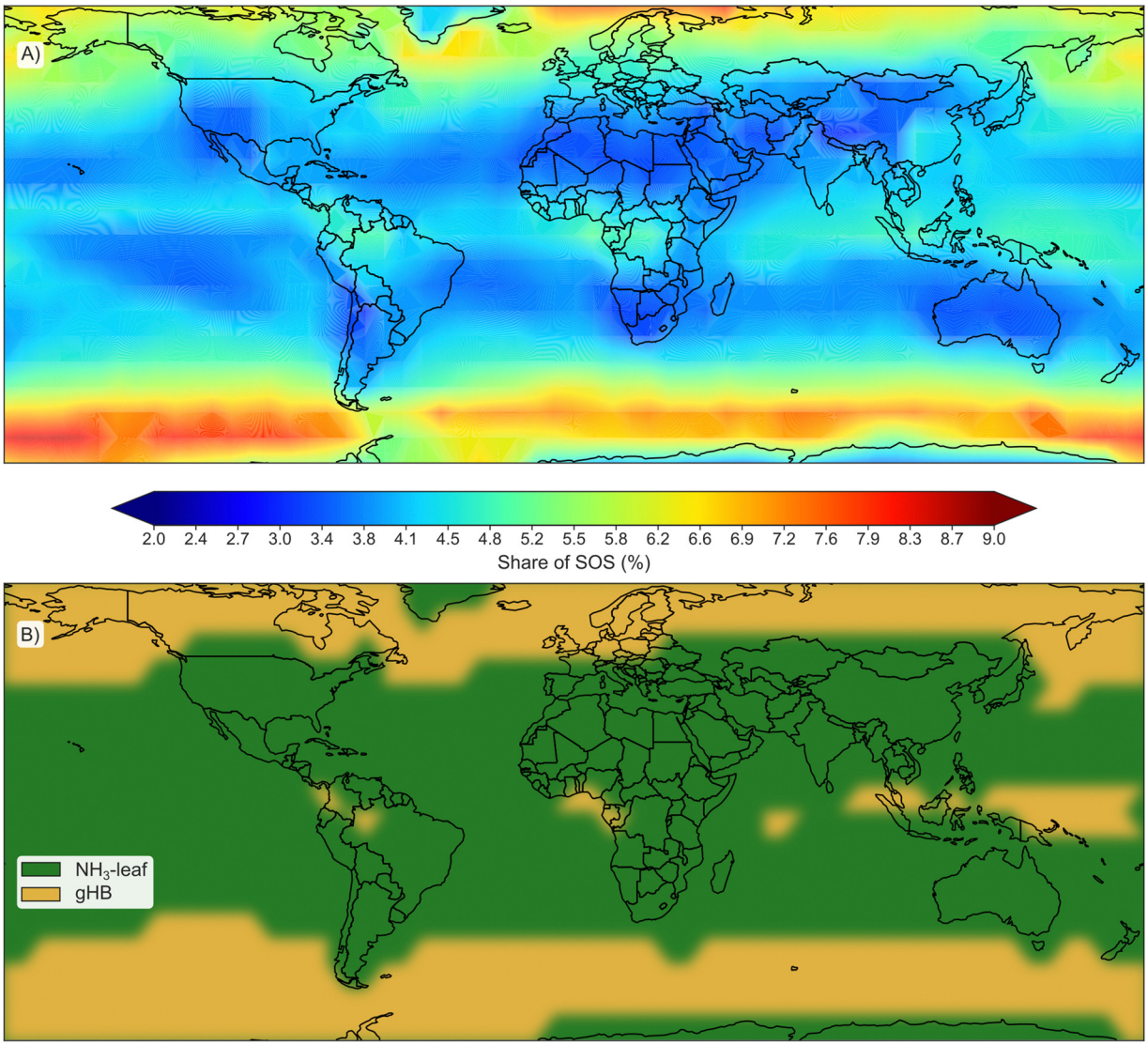

Fig. 8 World map showing the minimum impact on climate change – CO_2 concentration and the selection of the technology minimising the impact at each location considering two options: (i) ammonia leaf (NH_3-leaf) with 55% faradaic efficiency, and (ii) state-of-the-art green Haber–Bosch (gHB). (A) Minimum share of safe operating space (SOS) associated with the selected technology for each considered location. (B) Selected technology (green – NH_3-leaf and yellow – gHB) able to minimise the impact at each considered location.

We also highlight that the concept of NH_3-leaf technology herein analysed could be applicable to a nitrate-producing system (NO_3-leaf), drafted in Fig. S10 (ESI†). To do so, the ammonia produced in the cathodic chamber could be directed to the anode of the fuel cell, where a dedicated catalyst could oxidise it into nitrate. This scheme would be of high interest as nitrates are commonly used as fertilisers. However, the selective electrocatalytic oxidation of ammonia to nitrate is not yet developed, which makes this option a longer-term vision.

The geographical feasibility of the NH_3-leaf technology will expand, propelled by technological developments impacting solar panels, polymeric electrolyte membrane fuel cells, and electrolysers. Since they all contribute significantly to the CAPEX of an NH_3-leaf (Fig. 6A), it is of interest to summarise the main limitations they currently face. Solar panels are the most mature technology among the three ones. Nevertheless, materials and process engineering improvements are still demanded. Gains in solar-to-electricity efficiency must be accompanied by marked reductions in manufacturing costs to make it a direct competitor in the electricity market (*e.g.*, the new generation of benchmark monocrystalline Si modules must provide +2% efficiency with −50% cost).[108]

The development of polymeric electrolyte membrane fuel cells is still largely driven by materials and reactor design, in combination with incipient manufacturing optimization. Higher operation voltage by reducing cathodic losses, improved water and heat management, and removing the need of platinum-group metals as catalysts (which could drive to *ca.* 50% reduction of the manufacturing costs) are the main areas under investigation.[109,110] Regarding nitrogen electrolysers, the main limitations have been already sketched, including poor overall energy efficiency because of excessive anodic and

cathodic overpotentials and predominant production of hydrogen at the cathode, for which target values are given in Table 1. Optimization of manufacturing towards large scale production will become relevant at a further stage, but will expectedly benefit from experience accumulated for fuel cells or water electrolysers.

Conclusions

Here we conduct the first environmental and economic assessment of sustainable and decentralised ammonia production, revealing its potential to complement centralised strategies. We performed a spatially explicit analysis to investigate the potential of small-scale systems based on the electrocatalytic reduction of nitrogen (eN_2R) powered by photovoltaic energy (NH_3-leaf), comparing them with available technologies. Electrolysers showing *ca.* 30% energy efficiency – corresponding to 48% Faradaic efficiency under commonly reported conditions – would environmentally outperform the fossil Haber–Bosch process across all densely populated areas in the world. Attaining lower climate change impacts than its counterpart, the green Haber–Bosch process based on water electrolysis powered by PV would require a mild increase in energy conversion efficiencies from 21 to 29% at the sunniest locations. Similarly, reducing the human health damage of the fossil blue Haber–Bosch including CO_2 capture will require a similar 5% gain. Overall, location-dependent performance figures of merit suggest that a widespread implementation of the NH_3-leaf technology is feasible upon further efforts in catalyst and reactor design in eN_2R.

From the economic perspective, we determined the requirements to ensure the competence of the NH_3-leaf technology. Due to high capital costs and low technological maturity, the levelised cost of ammonia currently reachable is not competitive with fossil technologies based on the Haber–Bosch process. A combination of carbon tax schemes and the expected stark reduction in equipment costs as the technology matures may close the gap, highlighting the need for a combined action of policymakers and researchers.

Overall, our results quantifying the sustainability potential of the NH_3-leaf technology call for further research on this technology to develop a decentralised defossilised ammonia synthesis within the safe operating space while reducing human health impacts.

Data availability statement

The data relating to the figures and tables presented in this study are openly available in Zenodo under the DOI: **https://doi.org/10.5281/zenodo.7675514**. Additional data underlying this study are available from the corresponding author upon reasonable request.

Author contributions

SCD: conceptualisation, formal analysis, methodology, visualisation, writing – original draft, writing – review and editing; AM: conceptualisation, methodology, visualisation, writing – original draft, writing – review and editing; DFO: methodology, visualisation; SC: validation, review and editing; GGG: conceptualisation, writing – original draft, writing – review and editing, supervision, and project administration; and JPR: conceptualisation, writing – review and editing, supervision, and project administration.

Conflicts of interest

There are no conflicts to declare.

Acknowledgements

This publication was created as part of NCCR Catalysis (grant number 180544), a National Centre of Competence in Research funded by the Swiss National Science Foundation. SCD, AJM, GGG, and JPR are all authors affiliated with NCCR Catalysis.

References

1 J. Lim, C. A. Fernández, S. Woo Lee and M. C. Hatzell, *ACS Energy Lett.*, 2021, **6**, 3676–3685.
2 D. R. MacFarlane, P. V. Cherepanov, J. Choi, B. H. R. Suryanto, R. Y. Hodgetts, J. M. Bakker, F. M. Ferrero Vallana and A. N. Simonov, *Joule*, 2020, **4**, 1186–1205.
3 S. S. Rathore, S. Biswas, D. Fini, A. P. Kulkarni and S. Giddey, *Int. J. Hydrog. Energy*, 2021, **46**, 35365–35384.
4 M.-C. Chiong, C. T. Chong, J.-H. Ng, S. Mashruk, W. W. F. Chong, N. A. Samiran, G. R. Mong and A. Valera-Medina, *Energy Convers. Manage.*, 2021, **244**, 114460.
5 C. Mounaïm-Rousselle, P. Bréquigny, A. V. Medina, E. Boulet, D. Emberson and T. Løvås, in *Engines and Fuels for Future Transport*, ed. G. Kalghatgi, A. K. Agarwal, F. Leach and K. Senecal, Springer Singapore, Singapore, 2022, pp. 257–279.
6 B. Zincir, in *Clean Fuels for Mobility*, ed. G. Di Blasio, A. K. Agarwal, G. Belgiorno and P. C. Shukla, Springer Singapore, Singapore, 2022, pp. 171–199.
7 P. Akbari, C. D. Copeland and S. Tüchler, in AIAA SCITECH 2022 Forum, American Institute of Aeronautics and Astronautics, 2021.
8 The Royal Society, Ammonia: zero-carbon fertiliser, fuel and energy store, **https://royalsociety.org/topics-policy/projects/low-carbon-energy-programme/green-ammonia/**(accessed 9 August 2022).
9 British Petroleum, bp Statistical Review of World Energy 2021, London, 2021, **https://www.bp.com/content/dam/bp/business-sites/en/global/corporate/pdfs/energy-economics/statistical-review/bp-stats-review-2021-full-report.pdf**.
10 S. C. D'Angelo, S. Cobo, V. Tulus, A. Nabera, A. J. Martín, J. Pérez-Ramírez and G. Guillén-Gosálbez, *ACS Sustain. Chem. Eng.*, 2021, **9**, 9740–9749.
11 J. W. McArthur and G. C. McCord, *J. Dev. Econ.*, 2017, **127**, 133–152.

12 S. Ornes, *Proc. Natl. Acad. Sci. U. S. A.*, 2021, **118**, e2119584118.
13 L. Wang, M. Xia, H. Wang, K. Huang, C. Qian, C. T. Maravelias and G. A. Ozin, *Joule*, 2018, **2**, 1055–1074.
14 P. Tunå, C. Hulteberg and S. Ahlgren, *Environ. Prog. Sustain. Energy*, 2014, **33**, 1290–1297.
15 Y. Bicer, I. Dincer, G. Vezina and F. Raso, *Environ. Manage.*, 2017, **59**, 842–855.
16 J. R. Gomez, J. Baca and F. Garzon, *Int. J. Hydrog. Energy*, 2020, **45**, 721–737.
17 Y. Bicer and I. Dincer, *Int. J. Hydrog. Energy*, 2017, **42**, 21559–21570.
18 J. Nandenha, E. H. Fontes, R. M. Piasentin, F. C. Fonseca and A. O. Neto, *J. Fuel Chem. and Technol.*, 2018, **46**, 1137–1145.
19 L. Tock, F. Maréchal and M. Perrenoud, *Can. J. Chem. Eng.*, 2015, **93**, 356–362.
20 P. Wang, S. Wang, B. Wang, L. Shen and T. Song, *Fuel Process. Technol.*, 2022, **227**, 107126.
21 C. Rakousky, G. P. Keeley, K. Wippermann, M. Carmo and D. Stolten, *Electrochim. Acta*, 2018, **278**, 324–331.
22 M. Felgenhauer and T. Hamacher, *Int. J. Hydrog. Energy*, 2015, **40**, 2084–2090.
23 A. J. Martín and J. Pérez-Ramírez, *Joule*, 2019, **3**, 2602–2621.
24 S. Z. Andersen, V. Čolić, S. Yang, J. A. Schwalbe, A. C. Nielander, J. M. McEnaney, K. Enemark-Rasmussen, J. G. Baker, A. R. Singh, B. A. Rohr, M. J. Statt, S. J. Blair, S. Mezzavilla, J. Kibsgaard, P. C. K. Vesborg, M. Cargnello, S. F. Bent, T. F. Jaramillo, I. E. L. Stephens, J. K. Nørskov and I. Chorkendorff, *Nature*, 2019, **570**, 504–508.
25 H.-L. Du, M. Chatti, R. Y. Hodgetts, P. V. Cherepanov, C. K. Nguyen, K. Matuszek, D. R. MacFarlane and A. N. Simonov, *Nature*, 2022, 1–2.
26 A. J. Martín, T. Shinagawa and J. Pérez-Ramírez, *Chem*, 2019, **5**, 263–283.
27 B. Young, M. Krynock, D. Carlson, T. R. Hawkins, J. Marriott, B. Morelli, M. Jamieson, G. Cooney and T. J. Skone, *Int. J. Greenh. Gas Control.*, 2019, **91**, 102821.
28 S. Sadeek, T. L. Chan, R. Ramdath, A. Rajkumar, M. Guo and K. Ward, *Data Brief*, 2020, **30**, 105593.
29 M. Perčić, N. Vladimir, I. Jovanović and M. Koričan, *Appl. Energy*, 2022, **309**, 118463.
30 J. Osorio-Tejada, N. N. Tran and V. Hessel, *Sci. Total Environ.*, 2022, **826**, 154162.
31 F. Keller, R. L. Voss, R. P. Lee and B. Meyer, *Resour., Conserv. Recycl.*, 2022, **179**, 106106.
32 A. Anastasopoulou, R. Keijzer, B. Patil, J. Lang, G. van Rooij and V. Hessel, *J. Ind. Ecol.*, 2020, **24**, 1171–1185.
33 M. Wang, M. A. Khan, I. Mohsin, J. Wicks, A. H. Ip, K. Z. Sumon, C.-T. Dinh, E. H. Sargent, I. D. Gates and M. G. Kibria, *Energy Environ. Sci.*, 2021, **14**, 2535–2548.
34 G. Hochman, A. S. Goldman, F. A. Felder, J. M. Mayer, A. J. M. Miller, P. L. Holland, L. A. Goldman, P. Manocha, Z. Song and S. Aleti, *ACS Sustain. Chem. Eng.*, 2020, **8**, 8938–8948.
35 C. A. Fernandez and M. C. Hatzell, *J. Electrochem. Soc.*, 2020, **167**, 143504.
36 J. R. Gomez and F. Garzon, *Int. J. Energy Res.*, 2021, **45**, 13461–13470.
37 J. Lim, C. A. Fernández, S. Woo Lee and M. C. Hatzell, *ACS Energy Lett.*, 2021, **6**, 3676–3685.
38 CO_2 emission intensity—European Environment Agency, **https://www.eea.europa.eu/data-and-maps/daviz/co2-emission-intensity-5** (accessed 30 March 2022).
39 C. Zhao, M. Xi, J. Huo, C. He and L. Fu, *Mater. Today Phys.*, 2022, 100609.
40 S. Chatterjee, R. K. Parsapur and K.-W. W. Huang, *ACS Energy Lett.*, 2021, **6**, 4390–4394.
41 B. M. Comer, P. Fuentes, C. O. Dimkpa, Y. H. Liu, C. A. Fernandez, P. Arora, M. Realff, U. Singh, M. C. Hatzell and A. J. Medford, *Joule*, 2019, **3**, 1578–1605.
42 M. A. Mojid, G. C. L. Wyseure and S. K. Biswas, *J. Soil Sci. Plant Nutr.*, 2012, **12**, 655–665.
43 M. Fasihi, O. Efimova and C. Breyer, *J. Clean. Prod.*, 2019, **224**, 957–980.
44 E. Cetinkaya, I. Dincer and G. F. Naterer, *Int. J. Hydrog. Energy*, 2012, **37**, 2071–2080.
45 P. Heffer, A. Gruère and T. Roberts, Assessment of Fertilizer Use by Crop at the Global Level, International Fertilizer Association and International Plant Nutrition Institute, Paris, 2017.
46 HyLYZER®-200 HyLYZER®-250, **https://mart.cummins.com/imagelibrary/data/assetfiles/0070332.pdf** (accessed 30 March 2022).
47 X. Liu, A. Elgowainy and M. Wang, *Green Chem.*, 2020, **22**, 5751–5761.
48 R. D. Johnson, *NIST computational chemistry comparison and benchmark database*, National Institute of Standards and Technology, Gaithersburg, 2011.
49 G. Peng, J. Wu, M. Wang, J. Niklas, H. Zhou and C. Liu, *Nano Lett.*, 2020, **20**, 2879–2885.
50 B. H. R. Suryanto, H. L. Du, D. Wang, J. Chen, A. N. Simonov and D. R. MacFarlane, *Nat. Catal.*, 2019, **2**, 290–296.
51 A. Ursúa, L. Marroyo, E. Gubía, L. M. Gandía, P. M. Diéguez and P. Sanchis, *Int. J. Hydrog. Energy*, 2009, **34**, 3221–3233.
52 B. Parkinson, P. Balcombe, J. F. Speirs, A. D. Hawkes and K. Hellgardt, *Energy Environ. Sci.*, 2019, **12**, 19–40.
53 M. Gharibi and A. Askarzadeh, *Int. J. Hydrog. Energy*, 2019, **44**, 25428–25441.
54 A. Kraytsberg and Y. Ein-Eli, *Energy Fuels*, 2014, **28**, 7303–7330.
55 D. Xu, K. Li, B. Jia, W. Sun, W. Zhang, X. Liu and T. Ma, *Carbon Energy*, 2023, **5**, e230.
56 L. Fan, Z. Tu and S. H. Chan, *Energy Rep.*, 2021, **7**, 8421–8446.
57 S. K. Nabil, S. Mccoy and M. G. Kibria, *Green Chem.*, 2021, **23**, 867–880.
58 S. Budavari, M. O'Neal, A. Smith, P. Heckelman and J. Kinneary, *The Merck Index. An Encyclopedia of Chemicals, Drugs, and Biologicals*, Merck & Co., Whitehouse Station, NJ, 12th edn, 1996.
59 I. Ioannou, S. C. D'Angelo, A. J. Martín, J. Pérez-Ramírez and G. Guillén-Gosálbez, *ChemSusChem*, 2020, **13**, 6370–6380.

60 C. Brouwer and M. Heibloem, *Irrigation Water Management: Irrigation Water Needs*, Food and Agriculture Organisation, Rome, 2013, **https://www.fao.org/3/s2022e/s2022e00.html**.
61 K. K. Tanji, *Salinity: Environment-Plants-Molecules*, Springer, Dordrecht, 2002, pp. 21–51.
62 D. A. Notter, K. Kouravelou, T. Karachalios, M. K. Daletou and N. T. Haberland, *Energy Environ. Sci.*, 2015, **8**, 1969–1985.
63 C. S. Gittleman, A. Kongkanand, D. Masten and W. Gu, *Curr. Opin. Electrochem.*, 2019, **18**, 81–89.
64 M. Z. Jacobson and V. Jadhav, *Sol. Energy*, 2018, **169**, 55–66.
65 S. Pfenninger and I. Staffell, *Energy*, 2016, **114**, 1251–1265.
66 I. Staffell and S. Pfenninger, *Energy*, 2016, **114**, 1224–1239.
67 G. Wernet, C. Bauer, B. Steubing, J. Reinhard, E. Moreno-Ruiz and B. Weidema, *Int. J. Life Cycle Assess.*, 2016, **21**, 1218–1230.
68 International Organization for Standardization, ISO 14040:2006-Environmental management-Life Cycle Assessment: Principles and framework, ISO, 2014, **https://www.iso.org/standard/37456.html**.
69 International Organization for Standardization, ISO 14044:2006-Environmental management-Life Cycle Assessment: Requirements and guidelines, ISO, 2014, **https://www.iso.org/standard/38498.html**.
70 International Energy Agency, World Energy Outlook 2019, OECD Publishing, Paris, 2019, **https://doi.org/10.1787/caf32f3b-en**.
71 B. M. Campbell, D. J. Beare, E. M. Bennett, J. M. Hall-Spencer, J. S. I. Ingram, F. Jaramillo, R. Ortiz, N. Ramankutty, J. A. Sayer and D. Shindell, *Ecol. Soc.*, 2017, **22**, 8.
72 L. E. Apodaca, Mineral commodity summaries 2020: Nitrogen (fixed) - Ammonia, Lakewood, CO, 2020, **https://doi.org/10.3133/70202434**.
73 International Energy Agency, *Ammonia Technology Roadmap. Towards more sustainable nitrogen fertiliser production*, ed. J. French-Brooks, OECD Publishing, Paris, 2021, **https://www.iea.org/reports/ammonia-technology-roadmap**.
74 M. Goedkoop, M. Oele, J. Leijting, T. Ponsioen and E. Meijer, Introduction to LCA with SimaPro, PRé Sustainability, Amersfoort, 2016.
75 K. Bareiß, C. de la Rua, M. Möckl and T. Hamacher, *Appl. Energy*, 2019, **237**, 862–872.
76 S. Evangelisti, C. Tagliaferri, D. J. L. Brett and P. Lettieri, *J. Clean. Prod.*, 2017, **142**, 4339–4355.
77 L. Carrette, K. A. Friedrich and U. Stimming, *Chem. Phys. Chem.*, 2000, **1**, 162–193.
78 L. Bertuccioli, A. Chan, D. Hart, F. Lehner, B. Madden and E. Standen, Study on development of water electrolysis in the EU, Lausanne, Fuel Cell and Hydrogen Joint Undertaking, 2014.
79 M. Jouny, W. Luc and F. Jiao, *Ind. Eng. Chem. Res.*, 2018, **57**, 2165–2177.
80 H. Shin, K. U. Hansen and F. Jiao, *Nat. Sustain.*, 2021, **4**, 911–919.
81 J. Wyndorps, H. Ostovari and N. von der Assen, *Sustain. Energy Fuels*, 2021, **5**, 5748–5761.
82 W. Steffen, K. Richardson, J. Rockström, S. E. Cornell, I. Fetzer, E. M. Bennett, R. Biggs, S. R. Carpenter, W. De Vries, C. A. De Wit, C. Folke, D. Gerten, J. Heinke, G. M. Mace, L. M. Persson, V. Ramanathan, B. Reyers and S. Sörlin, *Science*, 2015, **347**, 1259855.
83 M. W. Ryberg, M. Owsianiak, K. Richardson and M. Z. Hauschild, *Ecol. Indic.*, 2018, **88**, 250–262.
84 Á. Galán-Martín, V. Tulus, I. Díaz, C. Pozo, J. Pérez-Ramírez and G. Guillén-Gosálbez, *One Earth*, 2021, **4**, 565–583.
85 M. M. Hanafiah, A. J. Hendriks and M. A. J. Huijbregts, *J. Clean. Prod.*, 2012, **37**, 107–114.
86 M. W. Ryberg, M. M. Andersen, M. Owsianiak and M. Z. Hauschild, *J. Clean. Prod.*, 2020, **276**, 123287.
87 M. A. J. Huijbregts, Z. J. N. Steinmann, P. M. F. Elshout, G. Stam, F. Verones, M. Vieira, M. Zijp, A. Hollander and R. van Zelm, *Int. J. Life Cycle Assess.*, 2017, **22**, 138–147.
88 G. Soloveichik, Renewable Energy to Fuels Through Utilization of Energy-Dense Liquids (REFUEL) Program Overview, U.S. Department of Energy, 2016, **https://arpa-e.energy.gov/technologies/programs/refuel**.
89 O. Edenhofer, R. Pichs Madruga, Y. Sokona, K. Seyboth, P. Eickemeier, P. Matschoss, G. Hansen, S. Kadner, S. Schlömer, T. Zwickel and C. Von Stechow, Renewable Energy Sources and Climate Change Mitigation: Special Report of the Intergovernmental Panel on Climate Change, Intergovernmental Panel on Climate Change, Cambridge, 2012.
90 X. Xue, R. Chen, C. Yan, P. Zhao, Y. Hu, W. Zhang, S. Yang and Z. Jin, *Nano Res.*, 2019, **12**, 1229–1249.
91 A. J. Martín, F. L. P. Veenstra, J. Lüthi, R. Verel and J. Pérez-Ramírez, *Chem Catalysis*, 2021, **1**, 1505–1518.
92 C. Guo, J. Ran, A. Vasileff and S.-Z. Qiao, *Energy Environ. Sci.*, 2018, **11**, 45.
93 E. Skúlason, T. Bligaard, S. Gudmundsdóttir, F. Studt, J. Rossmeisl, F. Abild-Pedersen, T. Vegge, H. Jónsson and J. K. Nørskov, *Phys. Chem. Chem. Phys.*, 2012, **14**, 1235–1245.
94 B. M. Ceballos, G. Pilania, K. P. Ramaiyan, A. Banerjee, C. Kreller and R. Mukundan, *Curr. Opin. Electrochem.*, 2021, **28**, 100723.
95 S. S. Rathore, S. Biswas, D. Fini, A. P. Kulkarni and S. Giddey, *Int. J. Hydrog. Energy*, 2021, **46**, 35365–35384.
96 T. Sterner, E. B. Barbier, I. Bateman, I. van den Bijgaart, A.-S. S. Crépin, O. Edenhofer, C. Fischer, W. Habla, J. Hassler, O. Johansson-Stenman, A. Lange, S. Polasky, J. Rockström, H. G. Smith, W. Steffen, G. Wagner, J. E. Wilen, F. Alpízar, C. Azar, D. Carless, C. Chávez, J. Coria, G. Engström, S. C. Jagers, G. Köhlin, Å. Löfgren, H. Pleijel and A. Robinson, *Nat. Sustain.*, 2019, **2**, 14.
97 Global health estimates: Disease burden by Cause, Age, Sex, by Country and by Region, 2000–2019, World Health Organization, Geneva, 2020, **https://www.who.int/data/gho/data/themes/mortality-and-global-health-estimates/global-health-estimates-leading-causes-of-dalys**.
98 R. W. Howarth and M. Z. Jacobson, *Energy Sci. Eng.*, 2021, **9**, 1676–1687.
99 M. C. Romano, C. Antonini, A. Bardow, V. Bertsch, N. P. Brandon, J. Brouwer, S. Campanari, L. Crema, P. E. Dodds, S. Gardarsdottir, M. Gazzani, G. Jan Kramer, P. D. Lund, N. Mac Dowell, E. Martelli, L. Mastropasqua, R. C. McKenna, J. G. M. S. Monteiro, N. Paltrinieri, B. G. Pollet, J. G. Reed, T. J. Schmidt, J. Vente and D. Wiley, *Energy Sci. Eng.*, 2022, **10**, 1944–1954.

100 M. L. Parisi, S. Maranghi, L. Vesce, A. Sinicropi, A. Di Carlo and R. Basosi, *Renew. Sust. Energ. Rev.*, 2020, **121**109703.
101 CO_2 emissions (kt)|Data, **https://data.worldbank.org/indicator/EN.ATM.CO2E.KT** (accessed 30 March 2022).
102 C. Smith, A. K. Hill and L. Torrente-Murciano, *Energy Environ. Sci.*, 2020, **13**, 331–344.
103 World Bank Group, Commodity Markets Outlook: Pandemic, war, recession: Drivers of aluminum and copper prices, October 2022, World Bank, Washington, DC, 2022, **https://openknowledge.worldbank.org/handle/10986/38160**.
104 Boston Consulting Group, How the EU Carbon Border Tax Will Redefine Value Chains|BCG, **https://www.bcg.com/publications/2021/eu-carbon-border-tax** (accessed 30 March 2022).
105 International Energy Agency, The Future of Hydrogen, OECD Publishing, Paris, 2019, **https://iea.blob.core.windows.net/assets/9e3a3493-b9a6-4b7d-b499-7ca48e357561/The_Future_of_Hydrogen.pdf**.
106 R. Rath, P. Kumar, S. Mohanty and S. K. Nayak, *Int. J. Energy Res.*, 2019, **43**, 8931–8955.
107 M. Xiao, T. Junne, J. Haas and M. Klein, *Energy Strateg. Rev.*, 2021, **35**, 100636.
108 C. Ballif, F. J. Haug, M. Boccard, P. J. Verlinden and G. Hahn, *Nat. Rev. Mater.*, 2022, **7**, 597–616.
109 Y. Wang, D. F. Ruiz Diaz, K. S. Chen, Z. Wang and X. C. Adroher, *Mater. Today*, 2020, **32**, 178–203.
110 Y. Wang, Y. Pang, H. Xu, A. Martinez and K. S. Chen, *Energy Environ. Sci.*, 2022, **15**, 2288–2328.

